Cell Adhesion

DOI: 10.1002/ange.201302048

Near-Infrared- and pH-Responsive System for Reversible Cell Adhesion using Graphene/Gold Nanorods Functionalized with i-Motif DNA**

*Wen Li, Jiasi Wang, Jinsong Ren, and Xiaogang Qu**

Cell adhesion plays a central role in multicellular organisms and disease because it is not only a physical link to the environment, but also can activate signaling pathways that have profound effects on cell fate and diverse physiological processes, including wound healing, tissue repair, and cancer metastasis.[1] Molecular approaches to control cell adhesion and migration hold considerable promise in tissue engineering, medical implantation and immunological response.[2] Recently, dynamic substrates that can mimic the characteristics of the natural extracellular matrix (ECM) and turn surface properties "on" or "off" with external stimulus have attracted much attention.[3] Thus far, the switchable surfaces have been engineered to respond to an electric field,[4] UV/Vis light,[5] temperature,[6] chemical stimuli,[7] enzymatic activities,[8] and magnetic field.[9] Among these stimuli, light is highly attractive as it allows control over the cells from a distance with relatively high spatial and temporal precision. To date, photoactivated cell adhesion usually requires modification of the cell-adhesion peptide arginine-glycine-aspartic acid (RGD) with a photolabile caging group[5a] and linkage of the RGD peptide to the surface by photoresponsive azobenzene units[5b–c] or photocleavable linkers.[5d] Although much progress has been made, all these studies use high-energy UV/Vis light for irradiation, which may hinder their use in vivo and for clinical applications because of the harmful side effects and poor tissue penetration of UV/Vis light.[1a] A near-infrared (NIR) light-responsive system for cell adhesion could overcome these problems, because NIR light can penetrate tissues with sufficient intensity and minimal damage.[10] However, the efficiency of this approach is limited by the low two-photon absorption cross-section of typical chromophores.[11] Recent advances in NIR-absorbing nanomaterials, such as gold nanostructures,[12] carbon nanostructures,[13] and a copper semiconductor,[14] could help solve this problem. These nanomaterials can convert NIR light into heat by the photothermal effect. Herein, by incorporating an NIR-responsive graphene/Au nanorod with thermoresponsive DNA, we achieved the controlled release of cells by NIR light.

DNA was used as a thermoresponsive linker to capture cells for the following reasons: first, when anchoring live cells, DNA has little influence on the viability of cells;[15] second, the responsive temperature of DNA can be easily adjusted by changing the sequence (which can be applied to various conditions); third, DNA, as a typical smart material,[16] may provide more flexible control over cells by combining NIR light with other stimuli. Recently, a DNA matrix has been applied to the design of cell arrays and selective release of target cells through enzymatic digestion or strand displacement.[17] However, there are still problems to overcome. For example, DNA-modified surfaces are often destroyed following enzymatic digestion and cannot be regenerated for the next cycle, but with cell-release through strand displacement, the cooperative hybridization process often takes too long, making the process slow. Therefore, more sophisticated routes for DNA-directed cell release are needed. DNA can reversibly switch between different conformations in a controllable manner with a particular stimulus.[18] Therefore, a more efficient and regenerative catch-and-release technique for cells can be made using various stimuli-modulated reversible conformational transitions of DNA. Herein, human telomeric G-rich DNA and C-rich DNA with repeats of GGGTTA and CCCTTA were used for cell immobilization because theit duplex DNA (dsDNA) form can be reversibly disassembled, both by temperature and pH conditions (C-rich DNA forms a quadruplex i-motif at slightly acidic pH[19]).

This is the first report of NIR- and pH-dual-controlled reversible cell catch-and-release (Scheme 1). An indium tin oxide (ITO) surface was modified with functionalized graphene, which acted as both an NIR-responsive nanoheater[13] and a biocompatible scaffold for cell growth.[20] Then, the graphene surface was modified with another NIR-absorbing substance, Au nanorods (AuNRs), which should further enhance the photothermal efficiency.[12c] After that, the dsDNA (sequences of C-rich DNA1 and G-rich DNA2 are shown in the Supporting Information, Table S1) was used as a linker for cell immobilization. Human umbilical vein endothelial cells (HUVEC) were used to study the feasibility of our design. To mediate cell adhesion, RGD was chosen as the bioadhesive ligand covalently conjugated on the 3′-terminus of G-rich DNA2. RGD can be specifically recognized by integrins, the major receptors for cell-ECM adhesion.[21] To control cell adhesion effectively, the inactive sites of the substrate must be resistant to nonspecific cell binding. Therefore, we used Tween 20, a common detergent and

[*] W. Li, J. Wang, Prof. J. Ren, Prof. X. Qu
Laboratory of Chemical Biology, Division of Biological Inorganic Chemistry, State Key Laboratory of Rare Earth Resource Utilization, Graduate School of the Chinese Academy of Sciences, Changchun Institute of Applied Chemistry, Chinese Academy of Sciences
Changchun, Jilin 130022 (China)
E-mail: xqu@ciac.jl.cn

[**] This work was supported by 973 Project (2011CB936004, 2012CB720602), and NSFC (21210002, 91213302, 21072182).

Supporting information for this article is available on the WWW under http://dx.doi.org/10.1002/anie.201302048.

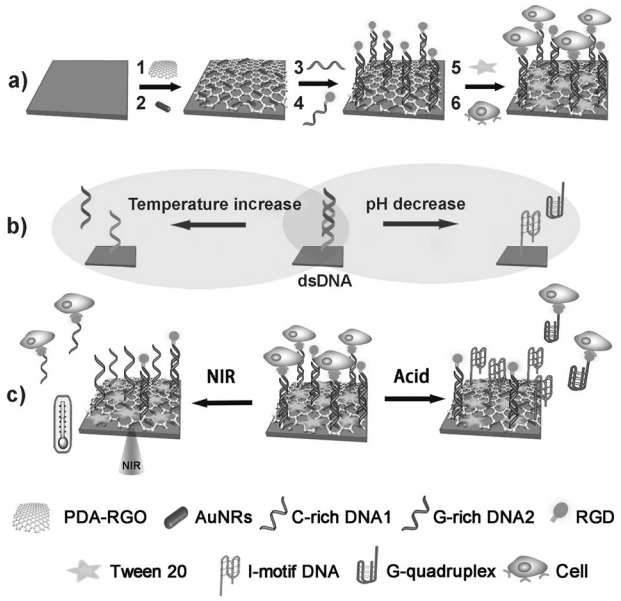

Scheme 1. A) Fabrication of a dual NIR- and pH-responsive substrate for cell adhesion. B) Temperature-dependent dissociation of dsDNA and pH-responsive conformation switching of i-motif DNA. C) Control of cell adhesion through NIR radiation and pH value.

blocking agent in bioanalytical assays, to minimize nonspecific cell adsorption. Tween 20 is composed of two parts: aliphatic ester chains that can prevent nonspecific cell binding and an aliphatic hydrocarbon chain that can easily adsorb on the graphene surface through hydrophobic interactions.[22] In our strategy, after exposure to NIR laser radiation, photoenergy was converted to heat by graphene and AuNRs. As a result, the dsDNA disassembled upon increasing temperature,[12b] and thus cells immobilized by the dsDNA linker would be detached from the surface. On the other hand, when the pH value was decreased, the C-rich DNA1 would fold into closed packed four-stranded structures, called i-motifs, and the duplex of dsDNA would dissociate.[19] Then, DNA2 would dissociate from the surface along with the cells. Because this procedure is not harmful to either the cells or the substrate, the system could be used for additional rounds of cell catch-and-release.

The substrate was fabricated as shown in Scheme 1 A. To avoid graphene aggregation and introduce more functional groups to the surface, dopamine (DA) was used both reduce and functionalize the graphene oxide (GO) in one step. Dopamine can self-polymerize into a polydopamine (PDA) coating on a wide range of substrates.[23] PDA is reactive with many groups, especially thiols and amines, thus conferring a facile method for immobilization of biomolecules such as DNA. Moreover, as a good reducing agent, dopamine can directly stabilize and reduce GO without using more hazardous hydrazine.[24] The PDA-capped reduced graphene oxide (PDA-RGO) was stable for several months (Supporting Information, Figure S1 a, inset). The reduction of GO by dopamine was monitored using UV/Vis absorption spectroscopy (Figure S1 a). In FT-IR spectra (Figure S1 b) of PDA-RGO, an absorption band at 3410 cm^{-1} (stretching vibration of catechol −OH groups) appeared, supporting the presence of PDA on the graphene.[25] Furthermore, under our experimental conditions, PDA-RGO showed no cytotoxicity when tested by MTT assay (Figure S1 d). After immobilizing PDA-RGO on the ITO surface, AuNRs, which can also absorb NIR photoenergy,[12] were adhered to the substrate to enhance the photothermal conversion efficiency. The AuNRs, with a longitudinal absorption band at 810 nm, were prepared (Figure S2) and immobilized on the surface using a Au-catechol interaction.[26] It has been reported that the interaction force between catechol and Au is comparable to that of streptavidin and biotin.[27] The prepared PDA-RGO modified ITO surfaces (PDA-RGO/ITO) were characterized by X-ray photoelectron spectroscopy (XPS; Figure S3 a), which showed the characteristic peaks of C1s, N1s, and O1s. Following the addition of AuNRs, a pair of peaks appeared at 87.7 eV and 88.1 eV, which were assigned to Au $4f_{7/2}$ and $4f_{5/2}$. XPS confirmed the immobilization of PDA-RGO and AuNRs on the ITO surface. The topography of the PDA-RGO/ITO with AuNRs was observed with SEM (Figure S3 b). For immobilization of the DNA linker, an amino-modified C-rich DNA1 was covalently linked to the surface by way of a Michael addition between the amine of DNA1 and the catechol group of PDA.[28] After that, the substrate was hybridized with the DNA2-RGD conjugate, forming dsDNA, and Tween 20 was added as a passivating agent, to minimize nonspecific cell binding.[22]

Following fabrication of the substrate, we focused on whether cells could be efficiently and specifically adhered to the surface. The substrate was seeded with HUVECs for three hours and monitored by microscopy. The HUVECs efficiently attached and spread on the surface with a fully extended morphology (Figure 1 a–c). Another surface was fabricated as a control using the same methods but without RGD. Limited cell adhesion was observed on the control surface and the cells exhibited a rounded morphology, indicating poor cell adhesion to the control surface (Figure 1 d). These results clearly indicated that Tween 20 could prevent nonspecific binding of cells and that cell adhesion was mediated by RGD.

ITO was chosen as the surface because it is conductive and therefore, suitable for electrochemical studies. Compared with other methods, electrochemistry is easy to perform and sensitive to changes in the surface properties.[29] Herein, we used cyclic voltammetry (CV) to trace each step of the synthesis of the substrate as well as cell adhesion. Typical CVs of $K_3[Fe(CN)_6]/K_4[Fe(CN)_6]$ with different ITO surfaces are shown in Figure 1 e. After modification of the surface with PDA-RGO and AuNRs, the peak current increased owing to their excellent conductivity (Figure S4 a). The current was almost constant, even after two days immersion in water, indicating the stable immobilization of PDA-RGO and AuNRs on the surface (Figure S4 b). In addition to CV, electrochemical impedance spectroscopy (EIS) is a highly sensitive method, which we used to track the immobilization with the change of electron transfer resistance (R_{et}).[30] ITO modified with PDA-RGO and AuNRs showed a low R_{et} value (Figure 1 f). After conjugation with DNA1 and subsequent hybridization with the DNA2-RGD, the R_{et} value increased because the negatively charged phosphate backbone repulsed the redox probe $[Fe(CN)_6]^{-3/-4}$ close to the electrode. Addition of insulating Tween 20 resulted in a further increase

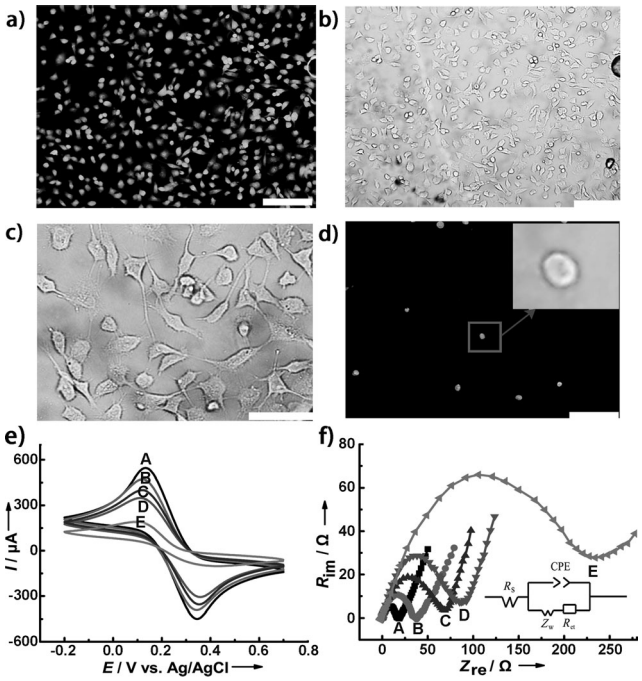

Figure 1. Microscopy images of HUVECs incubated on RGD-modified substrates: a) fluorescence image, b) corresponding bright field image, c) magnified bright field image. d) Cells were incubated on a control surface without RGD (inset: bright field image of one cell). Scale bars in (a, b, d) = 100 μm, scale bar in (c) = 50 μm. e) CVs and f) EIS of the AuNR-decorated PDA-RGO electrode (A), DNA1 linked to the substrate (B), hybridization of DNA2-RGD with DNA1 (C), surface blocked with Tween 20 (D), incubation of cells on the modified electrode (E). Inset: equivalent circuit.

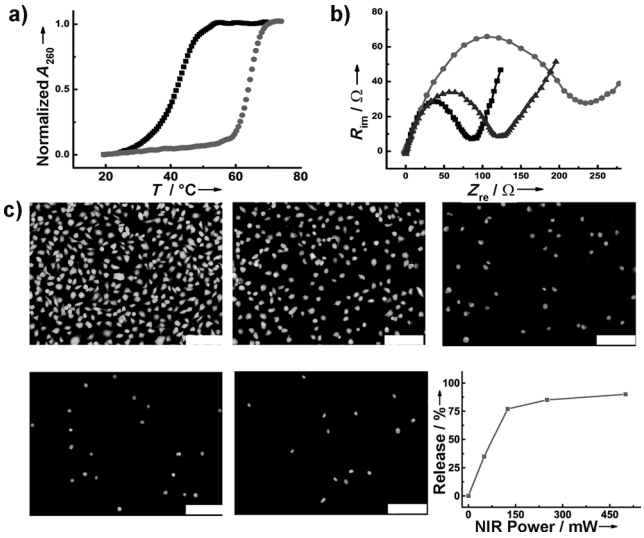

Figure 2. a) UV melting curves of dsDNA with three mismatched bases (black squares) and dsDNA with completely complementary sequence (gray circles). b) NIR-controlled cell release monitored by EIS; impedance spectra of modified electrode (squares), cell culture on the modified electrode (circles), and following NIR irradiation with 125 mW for 1 min (triangles). c) NIR-controlled cell release monitored by fluorescence microscopy: the power of the NIR irradiation was 0, 50, 125, 250, 500 mW, respectively. The graph shows the percentage of released cells versus NIR power. Scale bars = 100 μm.

in R_{et}. Finally, following incubation with cells, the R_{et} was greatly increased because access to the probe was blocked by the cells. The EIS results were consistent with those of CVs and suggested that the fabrication of the substrate was successful and the cells were adhering efficiently.

We also studied whether NIR light could release the adhered cells. Prior to examining this, it was necessary to evaluate the photothermal efficiency of graphene and AuNRs.[31] After exposure to an NIR laser of 808 nm, the change in the surface temperature was measured. Significant and rapid heating was observed, and the temperature changes increased with increasing laser intensity and irradiation time (Figure S5). In comparison, no temperature change was observed for the substrate without graphene and AuNRs or laser irradiation, under the same conditions. These results confirmed that graphene and AuNRs could heat the substrate using NIR radiation. Next, UV melting experiements were carried out to investigate the temperature-dependent dissociation of the dsDNA. The temperature at which a DNA duplex melts can be adjusted by changing the sequence and length of the duplex.[19c] Herein, to enhance the efficiency of cell release, we added three mismatched bases in the complementary region of dsDNA to decrease the melting temperature of the duplex. As shown in Figure 2a, the dsDNA we used had a melting temperature of 41.5 °C. Thus, it was stable at room temperature and did not require much energy to dissociate. To determine if the temperature-dependent dissociation of the dsDNA linker could mediate efficient cell release, we incubated the substrate at 45 °C. After one minute, cell release was easily observed. As heating continued, the amount of release increased and eventually plateaued (Figure S6). Finally, we monitored NIR-controlled cell detachment using electrochemical methods. After exposing the substrate to an 808 nm laser at 125 mW for one minute and washing gently, the corresponding R_{et} value decreased from 228 Ω to 125 Ω, suggesting that the amount of cells on the surface was greatly decreased, as anticipated (Figure 2b). In addition to EIS, fluorescence images were also used to visualize the cell release (Figure 2c). Prior to NIR exposure, the cells attached well on the surface. Over 75% of the original adherent cells were released from the surface following exposure to NIR radiation and the remaining cells displayed a round morphology. As the intensity of irradiation increased (Figure 2c) and the irradiation time increased (Figure S7), more cells were detached from the surface.

To verify that the NIR-triggered cell release was mediated by the photothermal effect, the substrates with graphene alone (Figure S8b), AuNRs alone (Figure S8c), and neither of the two (Figure S8d) were used as controls. After the same amount of NIR irradiation, few cells were removed from the substrates with graphene alone or AuNRs alone, and the release efficiency was significantly lower than that of the original substrate with both graphene and AuNRs (Figure S8a). As far as the substrate with neither of the two (Figure S8d), the cells were almost unaffected by NIR irradiation. These results confirmed that NIR irradiation alone does not affect cell adhesion, and the release observed was due to the photothermal effect of graphene and AuNRs. Additionally, to illustrate that the release of cells was due to dissociation of dsDNA, RGD peptides were immobilized

with a temperature-insensitive PEG linker, instead of dsDNA, and no significant cell release was observed following NIR irradiation (Figure S8e). Also, when a dsDNA with a melting temperature of 65 °C (Figure 2a) was used instead of the original three-base mismatched dsDNA (Figure S8f), following irradiation with the same light intensity, cells were not efficiently released from the surface, demonstrating that cell release was due to the temperature-dependent dissociation of the dsDNA.

For subsequent cell applications, it is better to efficiently release the cells with minimal influence on their viability. Finding a suitable power of NIR irradiation that can trigger cell release without damaging the cells is important. Although continuous NIR irradiation with high intensity could efficiently detach the cells, it could also overheat the cells, causing damage. Therefore, we tested a series of lasers with different power densities to determine the appropriate conditions. The viability of the released cells was evaluated using a live/dead assay. When the irradiation power was less than 125 mW, most of the released cells survived with a viability of about 88% (Figure S9a). However, the mortality of cells increased with higher laser power (Figure S9b). Taking the release efficiency and the cell viability into consideration, 125 mW was chosen for further studies.

Programmable techniques that can be used repeatedly for cell adhesion are promising. However, most of the reported methods cannot be reused because the original substrate is destroyed during the process. We examined whether our substrate could repeat the catch-and-release of cells. The photothermal stability of the substrate after laser irradiation was studied by SEM (Figure S10). Even after exposure to 125 mW CW laser for 15 minutes, no obvious morphology change of the substrate was observed. Next, fluorescence images were taken to monitor the cell catch-and-release for another two cycles (Figure S11). After the substrate was hybridized with DNA2-RGD for a second time, the cells once again attached to the substrate, and then the attached cells were released from the substrate with an additional round of NIR irradiation. After three cycles, a small decrease in efficiency was observed, which can be attributed to the unavoidable contamination of the substrate. These results clearly showed that the entire procedure was non-destructive and the substrate could be easily regenerated.

Our substrate also allows cell adhesion to be regulated by pH, which is important for flexible manipulation of cell behavior. Under slightly acidic conditions, C-rich DNA1 forms i-motifs, thus the dsDNA can dissociate resulting in cell release. We examined this pH-dependent DNA transition using CD spectroscopy. At pH 7.0, the DNA1 alone showed an unstructured single-stranded DNA spectrum (Figure S12a). When the pH was changed to 5.5, two CD bands characteristic of i-motif DNA (a positive band near 288 nm and a negative band near 256 nm) were observed.[19] We next confirmed that this pH-dependent transition of DNA1 could also happen from the dsDNA form (Figure 3a). The CD spectrum of dsDNA at pH 7.0 showed a positive peak near 263 nm and a negative peak near 240 nm, suggesting that C-rich DNA1 and G-rich DNA2 could hybridize to form a duplex under neutral conditions. At pH 5.5, the CD spectrum of the dsDNA was a combination of the spectra of an i-motif and a G-quadruplex (the spectral summation is shown in Figure S12b), which indicated that DNA1 and DNA2 were dissociated at pH 5.5 and formed their respective intramolecular quadruplex structures.[19c] An efficient conformational transition for the dsDNA under slightly acid conditions was aided by three mismatched bases within its complementary region, which facilitated duplex disassociation and conformational switching.

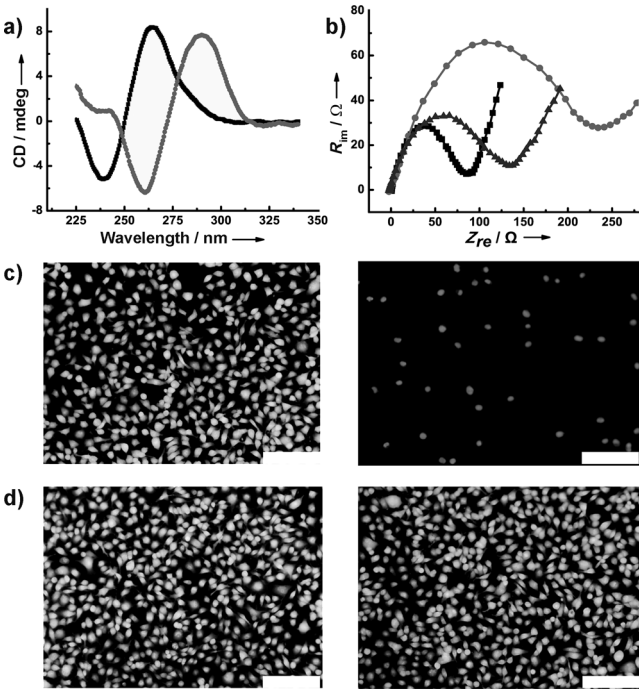

Figure 3. Controlled cell release by pH stimulus. a) CD spectra of dsDNA at pH 7.0 (black) or pH 5.5 (gray); b) cell release monitored by EIS: impedance spectra of the modified electrode (squares), cell culture on the modified electrode (circles), and the electrode after adjusting the pH to 5.5 for 8 min (triangles); fluorescence microscopy of c) cells on the modified substrate (left) and the substrate under acidic conditions (right); d) cells on the control substrate with pH-insensitive dsDNA (left) and the cells on the control substrate under acidic conditions (right).

We then studied pH-controlled cell release. At pH 7.0, the corresponding R_{et} value of the EIS curves was about 228 Ω owing to the large number of cells (Figure 3b). However, by adjusting the pH to 5.5 for eight minutes, the R_{et} decreased to 131 Ω, suggesting that most of the cells were released. Fluorescence images showed that the cells attached and occupied the whole substrate at pH 7.0. The cell coverage was significantly decreased under acidic conditions (Figure 3c). For a control experiment, a random dsDNA of the same length (which could not undergo a conformational transition with pH change) was used as the linker (Figure 3d). In this control, a negligible amount of cells were released at pH 5.5. This result confirmed that acidic conditions alone would not release the cells, and that the cell release was a result of the pH-dependent conformational switching of i-motif DNA.

The viability of the released cells was also evaluated using a live/dead cell assay. Fluorescence images (Figure S13) showed that most of the released cells were still alive,

indicating that the slightly acidic conditions used did not damage the cells. In addition, because of the reversibility of the i-motif conformation, the substrate was easily reused simply by adjusting the pH of the system. Fluorescence microscopy was used to trace reversible cell catch-and-release for two more cycles (Figure S14). Following a second hybridization with DNA2-RGD under neutral conditions, the cells attached to the substrate again for another cycle, and when the pH was changed to 5.5 for a second time, the cells were released from the substrate again.

In summary, we successfully fabricated a novel NIR and pH dual-responsive dynamic system for controlled catch-and-release of cells. Upon NIR exposure, graphene and AuNRs acted as nanoheaters to elevate the local temperature, resulting in dissociation of the dsDNA and releasing the adhered cells. Compared with previously used UV/Vis light to control cell adhesion, NIR light can penetrate tissues and cells with sufficient intensity and little damage, which is superior for further applications. Also, by using the reversible pH-dependent conformation switching of i-motif DNA, efficient catch-and-release of cells was also achieved through pH stimulus. By combining of the photothermal effect of graphene/AuNRs and conformational changes in DNA, our work could help give new insights into cell adhesion by using a substrate that integrates stimuli-responsive smart nanomaterials and multifunctional biomolecules.

Received: March 11, 2013
Published online: May 21, 2013

Keywords: cell adhesion · gold nanorods · graphene · G-quadruplexes · near-infrared light

[1] a) O. Guillame-Gentil, O. Semenov, A. S. Roca, T. Groth, R. Zahn, J. Voros, M. Zenobi-Wong, *Adv. Mater.* **2010**, *22*, 5443; b) E. S. Place, N. D. Evans, M. M. Stevens, *Nat. Mater.* **2009**, *8*, 457.

[2] M. Mrksich, *Chem. Soc. Rev.* **2000**, *29*, 267.

[3] a) P. M. Mendes, *Chem. Soc. Rev.* **2008**, *37*, 2512; b) T. Sada, T. Fujigaya, Y. Niidome, K. Nakazawa, N. Nakashima, *ACS Nano* **2011**, *5*, 4414; c) J. Robertus, W. R. Browne, B. L. Feringa, *Chem. Soc. Rev.* **2010**, *39*, 354.

[4] a) B. M. Lamb, M. N. Yousaf, *J. Am. Chem. Soc.* **2011**, *133*, 8870; b) C. C. A. Ng, A. Magenau, S. H. Ngalim, S. Ciampi, M. Hockalingham, J. B. Harper, K. Gaus, J. J. Gooding, *Angew. Chem.* **2012**, *124*, 7826; *Angew. Chem. Int. Ed.* **2012**, *51*, 7706; c) B. Wildt, D. Wirtz, P. C. Searson, *Nat. Methods* **2009**, *6*, 211.

[5] a) Y. Ohmuro-Matsuyama, Y. Tatsu, *Angew. Chem.* **2008**, *120*, 7637; *Angew. Chem. Int. Ed.* **2008**, *47*, 7527; b) J. Auernheimer, C. Dahmen, U. Hersel, A. Bausch, H. Kessler, *J. Am. Chem. Soc.* **2005**, *127*, 16107; c) D. B. Liu, Y. Y. Xie, H. W. Shao, X. Y. Jiang, *Angew. Chem.* **2009**, *121*, 4470; *Angew. Chem. Int. Ed.* **2009**, *48*, 4406; d) M. Wirkner, J. M. Alonso, V. Maus, M. Salierno, T. T. Lee, A. J. Garcia, A. del Campo, *Adv. Mater.* **2011**, *23*, 3907.

[6] S. Iwanaga, Y. Akiyama, A. Kikuchi, M. Yamato, K. Sakai, T. Okano, *Biomaterials* **2005**, *26*, 5395.

[7] H. Kaji, K. Tsukidate, T. Matsue, M. Nishizawa, *J. Am. Chem. Soc.* **2004**, *126*, 15026.

[8] L. Chen, X. L. Liu, B. Su, J. Li, L. Jiang, D. Han, S. T. Wang, *Adv. Mater.* **2011**, *23*, 4376.

[9] A. Ito, K. Ino, T. Kobayashi, H. Honda, *Biomaterials* **2005**, *26*, 6185.

[10] R. Weissleder, *Nat. Biotechnol.* **2001**, *19*, 316.

[11] G. He, L. Tan, Q. Zheng, P. N. Prasad, *Chem. Rev.* **2008**, *108*, 1245.

[12] a) H. Liu, D. Chen, L. Li, T. Liu, L. Tan, X. Wu, F. Tang, *Angew. Chem.* **2011**, *123*, 921; *Angew. Chem. Int. Ed.* **2011**, *50*, 891; b) J. Yang, X. Liu, Z. Liu, F. Pu, J. Ren, X. Qu, *Adv. Mater.* **2012**, *24*, 2890; c) A. F. Zedan, S. Moussa, J. Terner, G. Atkinson, M. S. El-Shall *ACS Nano* **2013**, *7*, 627.

[13] a) J. T. Robinson, S. M. Tabakman, Y. Liang, H. Wang, H. S. Casalongue, D. Vinh, H. Dai, *J. Am. Chem. Soc.* **2011**, *133*, 6825; b) B. Tian, C. Wang, S. Zhang, L. Feng, Z. Liu, *ACS Nano* **2011**, *5*, 7000; c) M. Li, X. J. Yang, J. Ren, K. Qu, X. Qu, *Adv. Mater.* **2012**, *24*, 1722.

[14] M. Zhou, R. Zhang, M. Huang, W. Lu, S. L. Song, M. P. Melancon, M. Tian, D. Liang, C. Li, *J. Am. Chem. Soc.* **2010**, *132*, 15351.

[15] S. C. Hsiao, A. K. Crow, W. A. Lam, C. R. Bertozzi, D. A. Fletcher, M. B. Francis, *Angew. Chem.* **2008**, *120*, 8601; *Angew. Chem. Int. Ed.* **2008**, *47*, 8473.

[16] a) N. C. Seeman, *Trends Biochem. Sci.* **2005**, *30*, 119; b) J. Bath, A. J. Turberfield, *Nat. Nanotechnol.* **2007**, *2*, 275.

[17] a) S. Reisewitz, H. Schroeder, N. Tort, K. A. Edwards, A. J. Baeumner, C. M. Niemeyer, *Small* **2010**, *6*, 2162; b) G. A. Kwong, C. G. Radu, K. Hwang, C. J. Y. Shu, C. Ma, R. C. Koya, B. Comin-Anduix, S. R. Hadrup, R. C. Bailey, O. N. Witte, T. N. Schumacher, A. Ribas, J. R. Heath, *J. Am. Chem. Soc.* **2009**, *131*, 9695; c) Z. Zhang, N. Chen, S. Li, M. R. Battig, Y. Wang, *J. Am. Chem. Soc.* **2012**, *134*, 15716.

[18] Y. Krishnan, F. C. Simmel, *Angew. Chem.* **2011**, *123*, 3180; *Angew. Chem. Int. Ed.* **2011**, *50*, 3124.

[19] a) X. Li, Y. Peng, J. Ren, X. Qu, *Proc. Natl. Acad. Sci. USA* **2006**, *103*, 19658; b) C. Wang, Z. Huang, Y. Lin, J. Ren, X. Qu, *Adv. Mater.* **2010**, *22*, 2792; c) C. Zhao, K. Qu, J. Ren, X. Qu, *Chem. Eur. J.* **2011**, *17*, 7013.

[20] T. R. Nayak, H. Andersen, V. S. Makam, C. Khaw, S. Bae, X. Xu, P. L. Ee, J. H. Ahn, B. H. Hong, G. Pastorinm, B. Ozyilmaz, *ACS Nano* **2011**, *5*, 4670.

[21] E. Ruoslahti, M. D. Pierschbacher, *Science* **1987**, *238*, 491.

[22] a) L. Feng, L. Wu, J. Wang, J. Ren, D. Miyoshi, N. Sugimoto, X. Qu, *Adv. Mater.* **2012**, *24*, 125; b) R. J. Chen, S. Bangsaruntip, K. A. Drouvalakis, N. W. S. Kam, M. Shim, Y. Li, W. Kim, P. J. Utz, H. Dai, *Proc. Natl. Acad. Sci. USA* **2003**, *100*, 4984.

[23] H. Lee, S. M. Dellatore, W. M. Miller, P. B. Messersmith, *Science* **2007**, *318*, 426.

[24] L. Q. Xu, W. J. Yang, K.-G. Neoh, E.-T. Kang, G. D. Fu, *Macromolecules* **2010**, *43*, 8336.

[25] B. Fei, B. Qian, Z. Yang, R. Wang, W. C. Liu, C. L. Mak, J. H. Xin, *Carbon* **2008**, *46*, 1795.

[26] H. Lee, K. Lee, I. K. Kim, T. G. Park, *Adv. Funct. Mater.* **2009**, *19*, 1884.

[27] H. Lee, N. F. Scherer, P. B. Messersmith, *Proc. Natl. Acad. Sci. USA* **2006**, *103*, 12999.

[28] H. O. Ham, Z. Liu, K. H. Lau, H. Lee, P. B. Messersmith, *Angew. Chem.* **2011**, *123*, 758; *Angew. Chem. Int. Ed.* **2011**, *50*, 732.

[29] a) Y. Xiao, A. A. Lubin, A. J. Heeger, K. W. Plaxco, *Angew. Chem.* **2005**, *117*, 5592; *Angew. Chem. Int. Ed.* **2005**, *44*, 5456; b) Y. Peng, X. Wang, Y. Xiao, L. Feng, C. Zhao, R. Ren, X. Qu, *J. Am. Chem. Soc.* **2009**, *131*, 13813.

[30] T. Kurkina, A. Vlandas, A. Ahmand, K. Kern, K. Balasubramanian, *Angew. Chem.* **2011**, *123*, 3794; *Angew. Chem. Int. Ed.* **2011**, *50*, 3710.

[31] a) E. Miyako, H. Nagata, K. Hirano, T. Hirotsu, *Angew. Chem.* **2008**, *120*, 3666; *Angew. Chem. Int. Ed.* **2008**, *47*, 3610; b) G. Liu, J. Kim, L. P. Lee, *Nat. Mater.* **2007**, *5*, 27; c) M. G. Roper, C. J. Easley, L. A. Legendre, J. A. C. Humphrey, J. P. Landers, *Anal. Chem.* **2007**, *79*, 129.

